

# Chemical evolution of starburst galaxies: How does star formation proceed?

M. Mouhcine<sup>1,2</sup> and T. Contini<sup>1,3</sup>

<sup>1</sup> Observatoire Astronomique de Strasbourg, 11, rue de l'Université, F-67000 Strasbourg, France.

<sup>2</sup> Division of Astronomy & Astrophysics, University of California, Los Angeles, CA 90095-1562, USA

<sup>3</sup> Laboratoire d'Astrophysique de l'Observatoire Midi-Pyrénées – UMR 5572, 14 avenue E. Belin, F-31400 Toulouse, France

Received; accepted

**Abstract.** We compute chemical evolution models to constrain the mode and the history of star formation in starburst galaxies as a whole, i.e. over a large range of mass and metallicity. To this end, we investigate the origin of the dispersion observed in the evolution of both nitrogen-to-oxygen abundance ratio and galaxy luminosity as a function of metallicity for a large sample of starburst galaxies. We find that the variation of the star formation efficiency, in the framework of continuous star formation models, produce a scatter equivalent to what is observed in the N/O versus O/H diagram for low-mass HII galaxies only. However, continuous star formation models are unable to reproduce i) the scatter observed for massive starburst and UV-selected galaxies in the N/O versus O/H relation, and ii) the scatter in the  $M_B$  versus O/H scaling relation observed for the whole sample of starburst galaxies. The dispersion associated with the distribution of N/O as a function of metallicity, for both low-mass and massive galaxies, is well explained in the framework of bursting star formation models. It is interpreted as a consequence of the time-delay between the ejection of nitrogen and that of oxygen into the ISM. These models also reproduce the spread observed in the luminosity-metallicity relation. Metal-rich spiral galaxies differ from metal-poor ones by a higher star formation efficiency and starburst frequency. Low-mass galaxies experienced a few bursts of star formation whereas massive spiral galaxies experienced numerous and extended powerful starbursts. Finally, we confirm previous claims (Contini et al. 2002) that UV-selected galaxies are observed at a special stage in their evolution. Their low N/O abundance ratios with respect to other starburst galaxies is well explained if they have just undergone a powerful starburst which enriched their ISM in oxygen.

**Key words.** galaxies: starburst – galaxies: abundances – galaxies: evolution

## 1. Introduction

Retrieving the star formation history of galaxies is essential for understanding galaxy formation and evolution. The chemical properties of galaxies are closely related to their star formation history, and can be considered like fossil records, enabling us to track the galaxy formation history up to the present.

At a given metallicity, the distribution of nitrogen-to-oxygen (N/O) abundance ratios shows a large dispersion, both at low and high metallicity (Pagel 1985; Coziol et al. 1999; Contini et al. 2002). Only part of this scatter is due to uncertainties in the abundance determinations, and the additional dispersion must therefore be accounted for by galaxy evolution models. Various hypothesis were discussed to be responsible for such a scatter (e.g., Kobulnicky & Skillman 1998). One scenario invokes the chemical “pollution” from the N-rich wind of Wolf-Rayet stars within the present starburst (Pagel, Terlevich & Melnick 1986). Indeed, small-scale abundance inhomogeneities are suspected in a few starburst galaxies (i.e.,

Walsh & Roy 1989, 1993; Thuan, Izotov & Lipovetsky 1996; Kobulnicky et al. 1997). These observations suggest that, under some conditions, the metals ejected by the massive stars can cool very quickly and pollute the surrounding ISM on short ( $\sim 10^6$  yr) timescales. However, such localized enrichment does not seem to occur in most of young starburst galaxies (Kobulnicky 1999; Oey & Shields 2000), even if these objects contain numerous Wolf-Rayet stars. Moreover, Kobulnicky & Skillman (1998) have shown that the hypothesis of localized chemical “pollution” cannot explain the scatter in N/O at a given metallicity. Another explanation for the dispersion in N/O at a given metallicity involves differing contributions from primary and secondary nitrogen, which essentially amounts to variations of the initial mass function (IMF) from galaxy to galaxy. Despite some claims of IMF variations with time and environment (e.g., Eisenhauer 2001), there is no compelling evidence that the IMF varies in local galaxies (Parker & Garmany 1993; Hill, Madore & Freedman 1994; Hunter et al. 1997). Preferential oxygen loss from galaxies with high N/O and more effective oxygen retention in galaxies with low N/O may be an additional explanation for producing N/O variations at constant

metallicity. This mechanism has been discussed extensively (e.g., Dekel & Silk 1986; De Young & Gallagher 1990). It has been invoked to avoid the overproduction of oxygen in low-mass galaxies (Esteban & Peimbert 1995), but observational evidence of the impact of differential galactic winds on galaxy properties is still lacking.

A natural explanation for the variation of N/O at constant metallicity might be a significant time delay between the release of oxygen and that of nitrogen into the ISM (e.g. Contini et al. 2002, and references therein), while maintaining a universal IMF and standard stellar nucleosynthesis. The “delayed-release” model assumes that star formation is an intermittent process in galaxies (Edmunds & Pagel 1978; Garnett 1990) and predicts that the dispersion in N/O is due to the delayed release of nitrogen produced in low-mass longer-lived stars, compared to oxygen produced in massive, short-lived stars.

There is a lot of observational evidence suggesting that the star formation history of galaxies has not been monotonic with time, but exhibits instead significant fluctuations. Galaxies in the Local Group are excellent examples showing a variety of star formation histories (see Grebel 2000 for a recent review). Further evidence for the “multiple-burst” scenario was recently found in massive starburst nucleus galaxies (Coziol et al. 1999; Schinnerer, Eckart & Boller 2000; Lançon et al. 2001; Alonso-Herrero et al. 2001; de Grijs, O’Connell & Gallagher 2001). Even the low-mass and less evolved HII galaxies seem to be formed of age-composite stellar populations indicating successive bursts of star formation (Mas-Hesse & Kunth 1999; Raimann et al. 2000).

In the framework of hierarchical galaxy formation models, large structures such as galaxies grow through the merging process of dark matter halos into larger and larger units. Somerville, Primack & Faber (2001) have shown that models in which burst of star formation are triggered by galaxy-galaxy mergers reproduce the observed comoving number density of bright high-redshift Lyman-break galaxies. Moreover, Kauffmann, Charlot & Balogh (2001) recently explored numerical models of galaxy evolution in which star formation occurs in two modes: a low-efficiency continuous mode, and a high-efficiency mode triggered by interaction with a satellite. With these assumptions, the star formation history of low-mass galaxies is characterized by intermittent bursts of star formation separated by quiescent periods lasting several Gyrs, whereas massive galaxies are perturbed on time scales of several hundred Myrs and thus have fluctuating but relatively continuous star formation histories.

Several chemical models have been developed in order to investigate the evolution of the N/O abundance ratio as a function of metallicity. However, most of these theoretical investigations focused on small-mass dwarf irregular and blue compact galaxies (e.g. Matteucci & Tosi 1985; Pilyugin 1992, 1993; Marconi, Matteucci & Tosi 1994; Olofsson 1995; Kobulnicky & Skillman 1998; Bradamante, Matteucci & D’Ercole 1998; Larsen, Sommer-Larsen & Pagel 2001). Only a few models were dedicated to massive spiral galaxies (Diaz & Tosi 1986; Tosi & Diaz 1990), and nothing has been done to investigate the chemical properties of star forming galaxies as a whole, i.e. over a large range of mass and metallicity.

The main objective of this paper is to investigate whether low-mass and massive starburst galaxies have different star formation histories using their chemical and photometric properties as observational constraints. Successful scenarios must be able to reproduce the dispersion for both scaling relations of starburst galaxies, namely N/O and absolute magnitude as a function of metallicity.

This paper is organized as follows. In Section 2 we summarize the observational constraints for the chemical properties of starburst galaxies. In Section 3 we describe the chemical and photometric evolution models used to reproduce the properties of galaxies, together with the nucleosynthesis prescriptions. The results are compared with the observational data and discussed in Section 4. Our principal conclusions are summarized in Section 5.

## 2. Observational constraints

For this work, we consider three samples of starburst galaxies: HII galaxies, Starburst Nucleus Galaxies (SBNGs) and a new sample of UV-selected galaxies. HII galaxies are mostly small-mass and metal-poor galaxies whereas SBNGs are more massive and metal-rich (see Coziol et al. 1999 for the dichotomy). The HII galaxy sample is a compilation of irregular and blue compact dwarf galaxy samples from Kobulnicky & Skillman (1996) and Izotov & Thuan (1999). The SBNG sample merges an optically selected sample (Contini, Considère & Davoust 1998; Considère et al. 2000) and a far-infrared selected sample (Veilleux et al. 1995). The sample of UV-selected starburst galaxies (Contini et al. 2002) spans a wide range of oxygen abundances, from  $\sim 0.1$  to  $1 Z_{\odot}$ . These objects are thus intermediate between low-mass HII galaxies and massive SBNGs.

The behavior of these starburst galaxies in the N/O vs. O/H plane (see Fig. 1) has already been investigated by Contini et al. (2002). At a given metallicity, the majority of UV-selected galaxies has low N/O abundance ratios whereas SBNGs show an excess of nitrogen abundance when compared to HII regions in the disk of normal galaxies (see also Coziol et al. 1999). The interpretation of these behaviors is not straightforward. Possible interpretations of the location of UV-selected galaxies and SBNGs in the N/O vs. O/H relation could be that UV galaxies are picked out at the end of a short episode of star formation following a rather long and quiescent period (Contini et al. 2002), whereas SBNGs experienced successive starbursts over the last Gyrs to produce the observed nitrogen abundance excess (e.g., Coziol et al. 1999)

The behavior of starburst galaxies in the luminosity–metallicity plane (see Fig. 2) has also been investigated by Contini et al. (2002). UV-selected and HII galaxies systematically deviate from the metallicity–luminosity relation followed by local “normal” galaxies, i.e. without active star formation. They appear to be 2 – 3 mag brighter than “normal” galaxies of similar metallicity, as might be expected if a strong starburst had temporarily lowered their mass-to-light ratios. Luminous ( $M_B \sim -20$ ) UV-selected galaxies behave like massive SBNGs, which show a significant departure from the metallicity–luminosity relation: they have higher metallicities than expected for their absolute  $B$ -band magnitudes. This be-

havior could be understood in the context of hierarchical galaxy formation (see Coziol et al. 1998). According to this scenario, galaxy bulges form first through violent mergers and disks form later, through accretion of residual outlying gas and/or small gas-rich galaxies. Following Struck-Marcell's (1981) models, accretion of more gas than stars will result in a steepening of the metallicity-luminosity relation, explaining the behavior of SBNGs and massive galaxies in general.

### 3. Chemical evolution models

#### 3.1. Assumptions

The chemical evolution is calculated by solving the usual set of differential equations for the gas mass density, chemical elements mass density and the total metallicity (e.g. Tinsley 1980). The model is fully described in Mouhcine & Lançon (2001a). We will recall here the relevant parameters of the model.

The evolution of the abundance  $X_i$  of element  $i$  in the interstellar medium obeys:

$$\frac{d(X_i M_{gas})}{dt} = -X_i \psi(t) + R_i(t) + X_{i,f} f(t) \quad (1)$$

where  $\psi(t)$  is the star formation rate,  $M_{gas}$  is the mass of the interstellar gas,  $f(t)$  is the gas infall rate, and  $X_{i,f}$  is the abundance of the infalling gas.  $R_i$  describes the rate of gas ejected from stars and returning into the ISM. It includes the enrichment from both single stars and close binary systems. Type Ia supernovae (hereafter SNe Ia) are assumed to originate in close binary systems in which one star at least is a C-O white dwarf (Whelan & Iben 1973), within the range of the binary masses  $3 M_\odot$  and  $16 M_\odot$ . The infall of gas from the companion pushes the mass about Chandrasekhar limit, triggering a deflagration with subsequent disruption of the star. SNe Ia could be considered since they contribute a large fraction of iron. The ejected stellar elements are assumed to be ejected at the end of the stellar life. Dynamical effects are not included in our models, we can not account for the internal structure of the ISM. We have to assume that the gas is always well mixed within the ISM. No instantaneous recycling is assumed which means that both the actual lifetime of each single star and the amount of ejected matter at that time are considered. Galactic winds are neglected and the whole galaxy is treated as a single unit from the beginning of its evolution. A one-phase interstellar medium is assumed. The lifetime and ejection rate of chemical elements is strongly dependent on the metallicity. In particular, the delayed enrichment by SNe Ia is taken into account following the prescriptions of Greggio & Renzini (1983).

The star formation rate is generally believed to be continuous with time. The most commonly used relation is a power-law, the so-called Schmidt law (Schmidt 1959). It assumes that the large-scale star formation rate scales with the gas density of the ISM ( $\psi \propto M_{gas}^k$ ), with the star formation efficiency as a free parameter. The efficiency is chosen such as to mimic the star formation histories along the Hubble sequence. In the literature, the value adopted for the exponent  $k$  varies between  $k = 1$  and 2. Recent observations by Kennicutt (1998) of the

correlation between the average star formation rate and surface densities in star-forming galaxies point towards an exponent of  $\sim 1.5$  in the Schmidt law. As long as such a law is assumed and the gas infall occurs continuously as a smooth function of time, the predicted star formation is also a smooth function of time.

The galaxy is assumed to be built by accretion of gas from the intergalactic medium. An exponential infall rate is assumed

$$f(t) = M_{tot} \frac{\exp(-t/\tau_f)}{\tau_f} \quad (2)$$

(Lacey & Fall 1985) where  $\tau_f$  is the gas accretion time scale for the galaxy formation, and  $M_{tot}$  is the total gas mass that can be accreted by the galaxy (i.e.,  $\int_0^\infty f(t) dt = M_{tot}$ ). Note that the adopted analytical formulae for the gas infall is arbitrary and that the most critical free parameter is the time scale of the gas infall. This expression is intended as a simple model with reasonable properties: a high rate at early stages of galaxy formation and a lower one at later stages. The gas accretion time scale has been assumed to be the same for all galaxy models. We assume that the accreted gas is primordial. The primordial gas abundances are taken from Walker et al. (1991).

We computed three types of models: models with continuous star formation in a closed box, models with continuous star formation and gas infall, and models assuming bursting star formation and gas infall.

The adopted star formation rate follows the Schmidt law for models with continuous star formation. When bursting models are considered, the star formation rate is given by:

$$\psi(t) = \begin{cases} \nu_s M_{gas}^k(t) & \text{if } t_j \leq t < t_j + \tau_B \\ 0 & \text{if } t_j + \tau_B \leq t \leq t_{j+1} \end{cases} \quad (3)$$

with  $t_{j+1} = t_j + \tau_B + \tau_{IB}$ , where  $t_j$  and  $t_{j+1}$  are the  $j^{\text{th}}$  and  $(j+1)^{\text{th}}$  burst starting time respectively,  $\tau_B$  is the burst duration, and  $\tau_{IB}$  is the interburst period.  $\nu_s$  is the star formation efficiency (expressed in unit of  $\text{Gyr}^{-1}$ ), and represents the inverse of the star formation timescale, namely the time necessary to consume all the available gas in the star-forming region. Each model is characterized by a fixed set of parameters (i.e.,  $T_{gal}$ ,  $\tau_B$ ,  $\nu_s$ ,  $\tau_{IB}$ ,  $\tau_f$ ,  $k$ ), where  $T_{gal}$  is the present-day age of the galaxy. In the rest of the paper we assume  $k = 1.5$ , and  $T_{gal} = 15 \text{ Gyr}$ .

Once the chemical evolution of a galaxy has been calculated, the evolution of its spectrophotometric properties can also be followed. To achieve this goal, population synthesis models of Mouhcine & Lançon (2001b) are used. The reader is referred to this paper for more details. These models span the range of metallicities  $1/50 \leq Z/Z_\odot \leq 2.5$ , and include all phases of stellar evolution relevant to the photometric evolution of galaxies: from zero-age main sequence to supernova explosion for massive stars, or to the end of the AGB phase for intermediate- and low-mass stars. Pre-main sequence and post-AGB are not accounted for in our population synthesis model as their contribution to the stellar population light budget and chemical enrichment is negligible. The evolutionary tracks up to the end of the early-AGB stars are those of the

Padova group (Bressan et al. 1993; Fagotto et al. 1994a,b). The extension to the end of the TP-AGB phase is constructed using AGB synthetic evolution models. The stellar spectral library of Lejeune et al. (1997) is used to achieve transformation of the theoretical quantities into observational ones. Nebular continuum emission is also included in the models. The nebular continuum emission coefficients in the infrared are taken from Ferland (1980) for HI and He II. Two-photon emission coefficients are taken from Brown & Mathews (1970). The number of ionizing photons is a fraction  $\beta$  of the number of Lyman continuum photons computed from our spectral library, while the rest is assumed to be absorbed by dust. We take  $\beta = 0.7$  as suggested from the measurements of HII regions in the LMC (DeGioia-Eastwood 1992).

### 3.2. Stellar yields

In this section we discuss the nucleosynthesis of heavy elements which are relevant to this study, namely nitrogen and oxygen. Furthermore, we state clearly at the outset that throughout our discussion we are considering only the most abundant isotope of each of these elements, i.e.,  $^{14}\text{N}$ , and  $^{16}\text{O}$ .

$^{14}\text{N}$  is a key element to understand the evolution of galaxies that have experienced successive starbursts since it needs relatively long time-scales ( $\sim 300$  Myr) to be ejected into the ISM. The origin of nitrogen has been a subject of debate for some years (Vila-Costas & Edmunds 1993). The basic nucleosynthesis process is well understood.  $^{14}\text{N}$  is produced mainly in the six steps of the CN branch of the CNO cycles within hydrogen burning stellar zones (see Cowley 1995 for a nucleosynthesis review). Nevertheless the type of star, with respect to mass, that dominate  $^{14}\text{N}$  production is not very well defined yet. Henry, Edmunds & Köppen (2000) have shown that intermediate-mass stars may be the main producer of  $^{14}\text{N}$ . Indeed, stars with initial masses in the range of  $3.5 - 4M_{\odot} \lesssim M_{\text{init}} \lesssim 6 - 8M_{\odot}$  (the upper limit is depending on details of the stellar evolution models) produce secondary  $^{14}\text{N}$  when the CN cycle operates in the bottom of their convective envelope for each third dredge-up event during the thermally pulsating AGB phase (Renzini & Voli 1981; van den Hoek & Groenewegen 1997; Marigo 2001; Mouhcine, in preparation). For these stars, models predict that the  $^{14}\text{N}$  production is increasing with metallicity. For low-mass stars ( $0.8M_{\odot} \lesssim M_{\text{init}} \lesssim 3 - 3.5M_{\odot}$ ), where no burning is operating at the bottom of their envelope, the ejecta is dominated by hydrogen and oxygen. However, AGB evolution models show clearly that intermediate-mass stars are not significant producers of  $^{16}\text{O}$ .

Regarding massive stars, it is well known that standard evolution models do not produce primary  $^{14}\text{N}$  (Woosley & Weaver 1995). However recent models taking into account the effect of rotation on the transport of chemical elements in the evolution of stellar interiors have revealed mechanisms for production of primary  $^{14}\text{N}$ . The helium convective shell would penetrate into the hydrogen layers, and consequently production of primary  $^{14}\text{N}$  may be efficient (Maeder 2000). Woosley & Weaver (1995) predict higher  $^{14}\text{N}$  production than Nomoto et al. (1997) at solar metallicity, and indicate that  $^{14}\text{N}$  production increases

with metallicity. Note that Maeder (1992) did not include the contribution from supernova ejection, only from stellar winds, in his derivation of nitrogen yields.

Maeder (1992) predicts a sizable decrease in  $^{16}\text{O}$  production with metallicity as the result of a mass-loss process which is metallicity sensitive (i.e.,  $\dot{M} \propto Z^{0.5}$ ), while Woosley & Weaver (1995) predict that they correlate directly with metallicity. Carigi (2000) have shown that the dependence of mass-loss on the metallicity for massive stars is crucial to match the observed behavior C/O radial distribution in the local Galactic disk, and hence she found that Maeder (1992) yields are more consistent with the data than Woosley & Weaver (1995) or Nomoto et al. (1997) stellar yields for the same stars.

For the chemical evolution models, we adopt the nucleosynthesis prescriptions from Maeder (1992) for massive stars, and from van den Hoek & Groenewegen (1997) for low- and intermediate-mass stars. For explosive nucleosynthesis products, we adopt the prescriptions by Thielemann et al (1986, model W7) for type Ia SNe, which we assume to originate from C-O white dwarfs in binary systems. This yield is assumed to be metallicity-independent, which is a reasonable assumption based upon the similarity of Thielemann et al's (1986)  $Z = Z_{\odot}$  and  $Z = 0$  models. The individual stellar lifetimes have been taken from evolutionary tracks of Padova group. Note that overshooting was used in the calculation of these tracks, meaning that the critical initial mass for supernova explosion will decrease compared to models which neglect overshooting. Finally, the IMF is truncated at  $0.1M_{\odot}$  and  $120M_{\odot}$ . In all our modeling, stars are distributed according to a Salpeter IMF (1955;  $\phi(m_i) \approx m_i^{-2.35}$ ).

## 4. Results

In order to understand the observed evolution and scatter in the N/O and luminosity vs. metallicity relations described in Section 2, we have computed several models considering both continuous and intermittent star formation histories. In our chemical evolution model, we decided to include only the well constrained ingredients in order to keep the number of free parameters as small as possible, to be confident in our interpretations. We assumed that the age zero for a galaxy corresponds to the moment when the first burst is occurring.

### 4.1. The N/O vs. O/H relation

Figure 1 (left panel) shows the distribution of N/O as a function of metallicity with the corresponding model predictions assuming continuous star formation histories with a star formation timescale ranging from 2 Gyr to 20 Gyr, and assuming that the galaxy forms via gas infall with timescale on the order of  $\tau_f = 1 - 7$  Gyr.

Chemical evolution models, assuming continuous star formation, are able to reproduce the general trend of the N/O vs. O/H relation. Different star formation efficiencies, typical of galaxies along the Hubble sequence (from irregulars to early-type spirals; Sandage 1986; Fioc & Rocca-Volmerange 1997; Lindner et al. 1999), are shown with different curves in Fig. 1. The general behavior of different models (i.e. using different

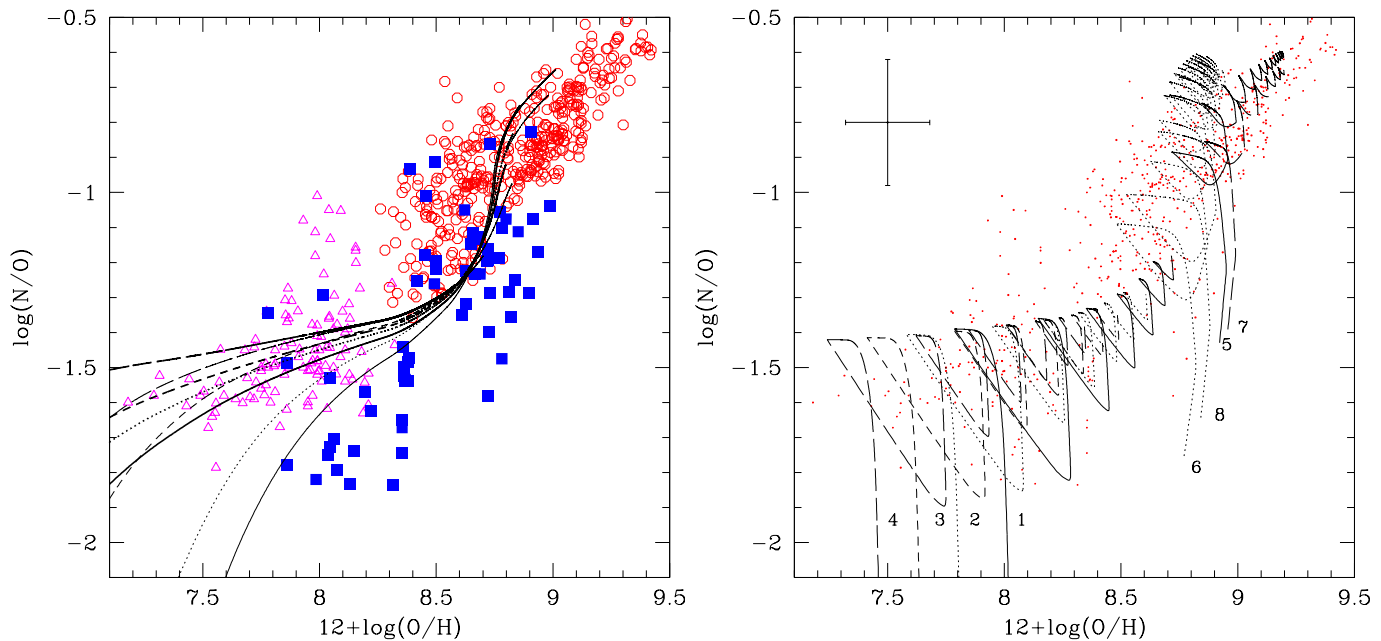


**Fig. 1.** N/O vs. O/H for a sample of UV-selected galaxies (squares), SBNGs (circles) selected in the optical or in the infrared, and HII galaxies (triangles). Typical uncertainties are shown in the upper left of the right panel. The left panel shows model predictions assuming a continuous star formation scenario with different star formation timescales  $\tau_{SF}$  (solid line:  $\tau_{SF} = 2$  Gyr, dotted line:  $\tau_{SF} = 3.5$  Gyr, short-dashed line:  $\tau_{SF} = 5$  Gyr, long-dashed line:  $\tau_{SF} = 20$  Gyr). The thick lines refer to models assuming an infall timescale  $\tau_f = 7$  Gyr, while thin lines refer to models with  $\tau_f = 4$  Gyr. The right panel shows model predictions assuming a bursting star formation scenario. The model parameters are listed in Table 1. This figure shows clearly the dichotomy between the models which reproduce the scatter in the metal-poor region ( $12 + \log(O/H) \leq 8.5$ ), and those which reproduce the scatter in the metal-rich region ( $12 + \log(O/H) \geq 8.5$ ).

SF efficiencies) is the same; the curves are simply shifted toward higher metallicities for higher star formation efficiencies. As expected, the models enter the plot at low metallicity values when the efficiency is low, i.e. a star formation efficiency typical of irregulars.

The N/O ratio rises steeply in the high-metallicity regime ( $12 + \log(O/H) \gtrsim 8.5$ ), because nitrogen synthesis in intermediate-mass stars is increasing with metallicity, while oxygen production in massive stars is decreasing. In this metallicity range, the N/O abundance ratio evolves more rapidly for high values of the star formation efficiency than for low ones. This behavior is related to the facts that i) the oxygen yield is decreasing with metallicity, and ii) the dilution of heavy elements due to gas infall is more efficient at high metallicity, for the simple reason that models calculated with a high star formation efficiency are metal-rich at younger ages. Increasing the gas infall rate affects the evolution of the N/O ratio in the sense that the same N/O value is achieved at lower metallicity for higher gas infall rate at a fixed star formation efficiency.

The models indicate that the behavior of low-metallicity galaxies ( $12 + \log(O/H) \lesssim 8.0$ ), located in the region where N/O is nearly constant with O/H, is naturally explained if these objects are characterized by low SFRs with a large fraction of N being produced by intermediate-mass stars (see also Legrand 2000; Henry et al. 2000). In this case, we do not need to assume that these galaxies are forming their first generation of stars.

Using closed-box models (i.e. without gas infall), the evolution of N/O as a function of metallicity is qualitatively similar to model predictions with gas infall, except that the predictions are scaled-up as no dilution by metal-free gas is operating.

Figure 1 (left panel) shows that, assuming a continuous star formation history, the systematic variation of the model parameters (i.e. star formation and gas infall timescales) may be a source of scatter in the N/O vs. O/H relation and could thus explain the behavior of low-mass HII galaxies. However, even considering a large range of free parameters, the predicted spread is much less than what is observed for metal-rich (i.e.,  $12 + \log(O/H) \gtrsim 8.5$ ) and UV-selected galaxies.

Theoretical predictions of selected models assuming a bursting star formation are shown in Fig.1 (right panel). Model parameters are summarized in Table 1. This plot shows the oscillating behavior of the N/O ratio due to the alternating bursting and quiescent phases. In this case, the observed dispersion in the N/O vs. O/H relation is explained by the time delay between the release of oxygen by massive stars into the ISM and that of nitrogen by intermediate-mass stars. During the starburst events, as massive stars dominate the chemical enrichment, the galaxy moves towards the lower right part of the diagram. During the interburst period, when no star formation is occurring, the release of N by low and intermediate-mass stars occurs a few hundred Myrs after the end of the burst and increases N/O at constant O/H. The dilution of interstellar gas

**Table 1.** Free parameters of selected bursting star formation models shown in Fig. 1 (right panel).  $\nu_s$  = star formation efficiency,  $\tau_B$  = starburst duration,  $\tau_{IB}$  = inter-burst period, and  $\tau_f$  = gas infall timescale. See text for more details.

	#	$\nu_s$ (Gyr $^{-1}$ )	$\tau_B$ (Myr)	$\tau_{IB}$ (Gyr)	$\tau_f$ (Gyr)
Region I	1	5	50	0.5	4
	2	3	50	0.5	4
	3	2	50	0.5	4
	4	1	50	0.5	4
Region II	5	25	100	1.0	1
	6	25	100	1.0	7
	7	25	100	2.0	1
	8	25	100	2.0	7

by the newly accreted intergalactic gas is also observed during the quiescent phases.

Model predictions with a bursting star formation were thus calculated with different sets of the model parameters. The burst duration was taken to vary from 10 Myr to 100 Myr. The interburst period varies from 0.5 Gyr to 7 Gyr, and the star formation efficiency varies from 0.5 Gyr $^{-1}$  to 30 Gyr $^{-1}$ . The number of bursts for each model is computed assuming that the galaxy end up with an age of 15 Gyr. The infall timescale varies from 1 Gyr to 7 Gyr. The difference between the models resides in the amount of massive stars formed during the burst which is increasing with increasing star formation efficiency, increasing burst duration, and decreasing gas infall timescale.

*One of the main goals of this study is to determine the range of values for the relevant model parameters that are able to reproduce both the mean evolution of N/O as a function of metallicity and its dispersion, and how these parameters depend on the galaxy type.*

The observed spread of N/O abundance ratio is quite well reproduced with the sets of parameters reported in Table 1. Extensive model computations show clearly that there is no possible combination of the model parameters (i.e.,  $\tau_B$ ,  $\nu_s$ ,  $\tau_{IB}$ ,  $\tau_f$ ) which would be able to account for the observed spread for the *whole sample* of galaxies. We found that the most important parameter for reproducing the observed spread is the star formation efficiency. Once the star formation efficiency is set, the extent of the predicted spread mainly depends on the starburst duration. The models show that to account for the observed scatter of N/O for the whole metallicity range, one needs to consider at least two *sets* of models characterized by different star formation efficiencies and starburst frequency (i.e. number of star formation events).

A closer look at the N/O vs. O/H diagram shows that there are two regions where the N/O abundance ratio evolves differently as a function of metallicity. The first region (hereafter region I) is occupied by galaxies with  $12 + \log(O/H) \lesssim 8.5$ . Those galaxies are mostly dwarf irregulars or metal-poor UV-selected galaxies. No correlation between N/O and O/H is seen for these galaxies. The second region (hereafter region II) is occupied by galaxies with  $12 + \log(O/H) \gtrsim 8.5$ . Most of them are SBNGs and metal-rich UV-selected galaxies. In this region

and in contrast to region I, galaxies with higher metallicity have also higher N/O ratio.

To reproduce the scatter observed in region I, one needs models assuming a relatively low star formation efficiency, between 0.5 and 5 Gyr $^{-1}$ . Burst durations on the order of  $\sim 10 - 100$  Myr are compatible with observations. Varying other free parameters has no significant effect on the model predictions. These models suggest that galaxies located in region I have experienced a few bursts ( $n_b \sim 1 - 4$ ) only. When these models enter into region II, they continue to show an oscillating behavior, but they produce lower scatter in the N/O vs. O/H diagram and have steeper evolution than what is observed in region II.

The second set of models, used to reproduce the scatter associated to region II, needs a much higher star formation efficiency (between 7 and 30 Gyr $^{-1}$ ) than what is needed to reproduce the scatter in region I. The models suggest that galaxies belonging to region II have experienced numerous (i.e.,  $n_b \sim 3 - 15$ ) and extended ( $\tau_B \simeq 60 - 100$  Myr) star formation events. We have found that a very good fit is provided by models for which the quiescent period between two successive bursts is of the same order as the gas infall timescale (i.e.,  $\tau_f \simeq \tau_{IB}$ ). This can be understood in the context of a hierarchical galaxy formation scenario where a major burst of star formation is activated each time a galaxy undergo a minor merger event, such as the accretion of a small satellite or primordial HI gas clouds.

The evolutionary status of UV-selected galaxies, recently discussed in Contini et al. (2002), may be understood in the framework of these models. Their low N/O abundance ratios, with respect to other starburst galaxies with comparable metallicities, is well explained if they have just undergone a powerful starburst which enriched their ISM in oxygen. In these objects nitrogen may have not been completely released.

#### 4.2. Metallicity-Luminosity relation

We now study the fundamental and well-known scaling relation between galaxy luminosity and metallicity (Contini et al. 2002 and references therein). This relation, which extends over  $\sim 10$  magnitudes in luminosity and  $\sim 2$  dex in metallicity seems to be an environmental (Vilchez 1995) and morphology-free (Aaronsen 1986, Mateo 1998) relation.

Richer & McCall (1995) and Hunter & Hoffman (1999) have reported that the dispersion in the metallicity of dwarf galaxies of comparable luminosity increases with decreasing luminosity. In addition to significant uncertainties in the abundance determinations (Hidalgo-Gómez & Olofsson 1998), the high surface brightness of the star-forming regions in dwarf galaxies may cause a deviation from the mean relation (Roennback & Bergvall 1995). Selective galactic winds and the fluctuations of the gas mass fraction among gas-rich dwarfs of a given luminosity (Pilyugin 2001) may also play a significant role to produce the observed scatter for these galaxies. However, a significant dispersion is also observed for massive and bright galaxies ( $M_B \lesssim -16$ ), for which the mechanisms invoked above are, in principle, not effective. Hence, one needs to

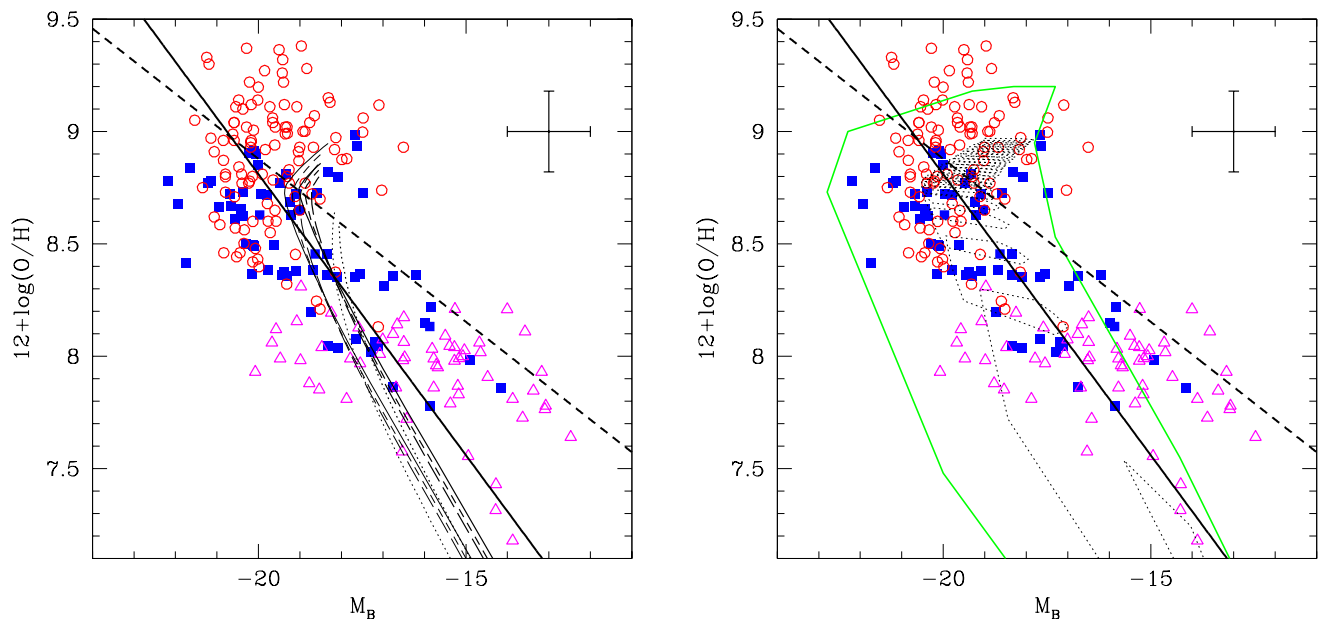


**Fig. 2.** The metallicity-luminosity relation for the starburst galaxy samples discussed in Section 2. Typical uncertainties are shown in the upper right of the right panel. The solid thick line is a linear fit to the whole sample of starburst galaxies, and the dashed thick line is a linear fit to local “normal” irregular and spiral galaxies (Kobulnicky & Zaritsky 1999). The left panel shows model predictions assuming a continuous star formation scenario (see Fig. 1 for the legend). The right panel shows predictions assuming a bursting star formation scenario. The model parameters are the same as those used in Fig. 1. The delineated area (thick line) encompasses all the model predictions calculated with the parameters reported in Table 1. For illustration, the prediction of a specific model (dotted thin line) is shown.

come up with other mechanism(s) to account for the observed scatter in the latter galaxies.

Using the chemo-photometric evolution models discussed in the previous section, we now examine how much scatter affecting the metallicity-luminosity relation can be predicted. Note that proceeding in such a way to reproduce the metallicity-luminosity relation and its associated scatter, means implicitly that the relation under study is caused by the ability of galaxies to produce metals, rather than their ability to keep the products of their own evolution. In the left panel of Figure 2, we show the evolution of the metallicity as a function of the  $B$ -band absolute magnitude assuming continuous star formation. The model parameters and data samples are those discussed in the previous section (see Fig. 1–left panel). Also shown are i) the linear fit to the whole sample of starburst galaxies (thick solid line) given by the following relation:  $12 + \log(O/H) = -0.25(\pm 0.01) \times M_B + 3.81(\pm 0.2)$ , and ii) a linear fit to the normal irregular and spiral galaxies (Kobulnicky & Zaritsky 1999).

The left panel of Figure 2 shows that models assuming continuous star formation are able to reproduce the “mean” relation between galaxy metallicity and luminosity. However, this plot shows that these models delineate a narrow region in the  $O/H$  vs.  $M_B$  diagram, even if the free parameters were taken to span a quite large range of values. Hence, the plot tells us that continuous star formation models are unable to account for the observed scatter affecting the metallicity-luminosity relation.

In the right panel of Figure 2, we show the evolution of metallicity as a function of the  $B$ -band absolute magnitude, assuming that the star formation proceeds in successive bursts. The delineated area (thick line) in the  $O/H$  vs.  $M_B$  plane encompasses all the model predictions calculated with the parameters reported in Table 1. For illustration, the prediction of a specific model (dotted thin line) is plotted in more details. When the star formation is active, the  $B$ -band magnitude and the oxygen abundance increase simultaneously, as a consequence of the presence of hot massive stars, responsible for the major fraction of the  $B$ -band light, and of supernova explosions which enrich the star-forming region in heavy elements. During this phase the galaxy evolves along the left-hand boundary of the allowed area. During the interburst period, the  $B$ -band magnitude and the oxygen abundance decrease due to the star formation inactivity and to the dilution of the interstellar gas by the metal-free gas infall. During this period, the galaxy evolves along the right-hand boundary of the allowed area. As the galaxy evolves, each starburst event consumes gas with enhanced element abundances in comparison to previous starburst events, leading to the intermittence between the two boundaries of the delineated area.

Figure 2 shows that the extent of the area allowed by intermittent star formation models is comparable to the observed spread of metallicity among galaxies of comparable luminosity. More appropriate constraints on how the star formation proceeds in starburst galaxies, and which are their basic scaling

relations may be derived using the N/H vs.  $M_K$  relation rather than O/H vs.  $M_B$ . Indeed, nitrogen is less sensitive to the recent star formation history of galaxies than oxygen. The same is true for the magnitude as the  $B$ -band is heavily affected by the most recent burst of star formation, and thus depend strongly on the evolutionary state of the galaxy. Near-infrared magnitudes will be more appropriate as a luminosity/mass indicator since it traces the total stellar mass of a galaxy (Contini, Mouhcine & Davoust, in preparation).

## 5. Summary and conclusions

We developed a chemical evolution model aimed at constraining the star formation history of starburst galaxies by investigating the origin of the dispersion observed in the evolution of both the N/O abundance ratio and galaxy luminosity as a function of metallicity. One of the main goals was to determine the range of values for the relevant model parameters characterizing the star formation history of starburst galaxies as a whole, i.e. over a large range of mass and metallicity.

The results of this investigation can be summarized as follows. The comparison of model predictions with the available data samples on the abundance ratios of heavy elements such as O and N allows us to conclude that continuous star formation models can reproduce the scatter in the N/O versus O/H relation observed for low-mass HII galaxies as a consequence of the systematic variation of the star formation efficiency among galaxies. However, continuous star formation models are unable to reproduce i) the scatter observed for massive starburst and UV-selected galaxies in the N/O versus O/H relation and ii) the scatter in the  $M_B$  versus O/H scaling relation observed for the whole sample of starburst galaxies.

The dispersion associated to the distribution of N/O as a function of metallicity is well explained in the framework of bursting star formation models. It is interpreted as a consequence of the time-delay between the ejection of nitrogen and that of oxygen into the ISM. We found that metal-rich galaxies differ from metal-poor ones by their star formation efficiency and starburst frequency. Indeed to match the observed mean evolution of N/O with metallicity and its dispersion for galaxies with  $12 + \log(O/H) \leq 8.5$ , the models suggest that their star formation efficiency need to be low (between 0.5 and  $5 \text{ Gyr}^{-1}$ ), with a small number of star formation events. On the contrary, the observed spread for galaxies located in the area where  $12 + \log(O/H) \gtrsim 8.5$ , is best reproduced with models assuming a higher star formation efficiency (between 7 and  $25 \text{ Gyr}^{-1}$ ), and more starburst events than metal-poor galaxies. We note also that only extended bursts ( $\sim 50 - 100 \text{ Myr}$ ) are compatible with the properties of massive metal-rich galaxies.

Bursting star formation models accounting for the observed scatter in the N/O vs. O/H diagram delineate an area in  $M_B$  vs. O/H diagram where galaxies need to fall. Good agreement is found with the location of data in this diagram.

*Acknowledgements.* We thank R. Coziol and E. Davoust for useful suggestions.

## References

- Aaronson M., 1986, in *Star Forming Dwarf Galaxies and Related Objects*, D. Kunth, T.X. Thuan & J.T.T. Van (eds.), Editions Frontières, p. 125
- Alonso-Herrero A., Engelbracht C.W., Rieke M.J., Rieke G.H., Quillen A.C., 2001, ApJ, 546, 952
- Bradamante F., Matteucci F., D’Ercole A., 1998, A&A 337, 338
- Bressan A., Fagotto F., Bertelli G., Chiosi C., 1993, A&AS 100, 647
- Brown R.L., Mathews W.G. 1970, ApJ 160, 939
- Carigi L., 2000, RMxAA, 36, 171
- Considère S., Coziol R., Contini T., Davoust, E., 2000, A&A, 356, 89
- Contini T., Considère S., Davoust E., 1998, A&AS, 130, 285
- Contini T., Treyer, M.-A., Sullivan M., Ellis R.S., 2002, MNRAS, 330, 75
- Cowley, C. R. 1995, *An introduction to cosmochemistry* (Cambridge: Cambridge Univ. Press)
- Coziol R., Contini T., Davoust E., Considère S., 1998, ASP Conf. Ser. 147: Abundance Profiles: Diagnostic Tools for Galaxy History, p. 219
- Coziol R., Reyes R. E. C., Considère S., Davoust E., Contini T., 1999, A&A, 345, 733
- de Grijs R., O’Connell R.W., Gallagher J.S., 2001, AJ, 121, 768
- De Young D.S., Gallagher J.S., 1990, ApJ, 356, L15
- DeGioia-Eastwood K., 1992, ApJ 397, 542
- Dekel A., Silk J., 1986, ApJ, 303, 39
- Diaz A.I., Tosi M., 1986, A&A, 158, 60
- Edmunds M.G., Pagel B.E.J., 1978, MNRAS, 185, 777
- Eisenhauer F., 2001, in *Starburst: Near and Far*, Tacconi L., Lutz D. (eds.), in press (astro-ph/0101321)
- Esteban C., Peimbert M., 1995, A&A 300, 78
- Fagotto F., Bressan A., Bertelli G., Chiosi C., 1994a, A&AS 105, 29
- Fagotto F., Bressan A., Bertelli G., Chiosi C., 1994b, A&AS 105, 39
- Ferland G.J., 1980, PASP 92, 596
- Fioc M., Rocca-Volmerange B., 1997, A&A, 326, 950
- Garnett D.R., 1990, ApJ 363, 142
- Grebel K., 2000, in *Evolution of Galaxies. I. Observational Clues*, J.M. Vilchez, G. Stasinska & E. Perez (eds.), Kluwer, Dordrecht, in press (astro-ph/0011048)
- Greggio L., Renzini A., 1983, A&A, 118, 217
- Henry R.B.C., Edmunds M.G., Köppen J., 2000, ApJ, 541, 660
- Hidalgo-Gómez A.M., Olofsson K., 1998, A&A 334, 45
- Hill R.J., Madore B.F., Freedman W.L., 1994, ApJ, 429, 204
- Hunter D.A., Hoffman L., 1999, AJ 119, 2789
- Hunter D.A., Light R.M., Holtzman J.A., Lynds R., O’Neil E.J., Grillmair C.J., 1997, ApJ, 478, 124
- Izotov Y. I., Thuan T. X., 1999, ApJ, 511, 639
- Kauffmann G., Charlot S., Balogh M.L., 2001, ApJ, in press (astro-ph/0103130)
- Kennicutt R.C., 1998, ApJ, 498, 541
- Kobulnicky H.A., 1999, IAU Symp. 193: Wolf-Rayet Phenomena in Massive Stars and Starburst Galaxies, 193, p. 670
- Kobulnicky H.A., Skillman E.D., 1996, ApJ, 471, 211
- Kobulnicky H.A., Skillman E.D., 1998, ApJ, 497, 601
- Kobulnicky H.A., Zaritsky D., 1999, ApJ, 511, 118
- Kobulnicky H.A., Skillman E.D., Roy J., Walsh J.R., Rosa M.R., 1997, ApJ, 477, 679
- Lacey C.G., Fall S.M., 1985, ApJ, 290, 154.
- Laçon A., Goldader J.D., Leitherer C., Delgado, R.M.G., 2001, ApJ, 552, 150
- Larsen T. I., Sommer-Larsen J., & Pagel B. E. J., 2001, MNRAS, 323, 555
- Legrand F., 2000, A&A, 354, 504
- Lejeune T., Cuisinier F., Buser R., 1997, A&AS 125, 229
- Lindner U., Fritze -von Alvensleben U., Fricke K.J., 1999, A&A 341, 709



- Maeder A., 1992, A&A, 264, 105  
Maeder A., 2000, New Astronomy Review, 44, 291  
Marconi G., Matteucci F., Tosi M., 1994, MNRAS, 270, 35  
Marigo P., 2001, A&A, 313, 545  
Mas-Hesse J.M., Kunth D., 1999, A&A, 349, 765  
Mateo M., 1998, ARA&A, 36, 435  
Matteucci F., & Tosi M., 1985, MNRAS, 217, 391  
Mouhcine M., Lançon A., 2001a, A&A, submitted  
Mouhcine M., Lançon A., 2001b, A&A, in press  
Nomoto K., Hashimoto M., Tsujimoto T., Thielemann F.-K.,  
Kishimoto N., Kubo Y., Nakasato N., 1997, Nucl. Phys. A, 616,  
79c  
Oey M.S., Shields, J.C., 2000, ApJ, 539, 687  
Olofsson K., 1995, A&A, 293, 652  
Pagel B.E.J., 1985, in *Production and Distribution of CNO Elements*,  
ed. I.J. Danziger, F. Matteucci, and K. Kjr., p. 155.  
Pagel B.E.J., Terlevich R.J., Melnick J., 1986, PASP 98, 1005  
Parker J.W., Garmany C.D., 1993, AJ, 106, 1471  
Pilyugin, L.S., 1992, A&A, 260, 58  
Pilyugin, L.S., 1993, A&A, 277, 42  
Pilyugin L.S., 2001, A&A, 374, 412  
Raimann D., Storchi-Bergmann T., Bica E., Melnick J., Schmitt H.,  
2000, MNRAS, 316, 559  
Renzini A., Voli M., 1981, A&A, 94, 175  
Richer M.G., McCall M.L., 1995, ApJ, 445, 642  
Roennback J., Bergvall N., 1995, A&A 302, 353  
Salpeter E.E., 1955, ApJ, 121, 161  
Sandage A., 1986, A&A 161, 89  
Schinnerer E., Eckart A., Boller T., 2000, ApJ, 545, 205  
Schmidt M., 1959, ApJ, 129, 243  
Somerville R.S., Primack J.R., Faber S.M., 2001, MNRAS 320, 504  
Struck-Marcell C., 1981, MNRAS, 197, 487  
Thielemann F.K., Nomoto K., Yohoi K., 1986, A&A, 158, 17  
Thuan T.X., Izotov Y.I., Lipovetsky V.A., 1996, ApJ, 463, 120  
Tinsley B.M., 1980, Fundam. Cosmic Phys., 5, 287  
Tosi M., Diaz A.I., 1990, MNRAS 246, 616  
van den Hoek L.B., & Groenewegen M.A.T., 1997, A&AS, 123, 305  
Veilleux S., Kim D., Sanders D. B., Mazzarella J. M., Soifer B. T.,  
1995, ApJS, 98, 171  
Vila-Costas M.B., & Edmunds M.G., 1993, MNRAS, 265, 199  
Vilchez J.M., 1995, AJ, 110, 1090  
Walker T.P., Steigman G., Kang H., Schramm D.M., Olive K.A., 1991,  
ApJ, 376, 51  
Walsh J.R., Roy J., 1989, MNRAS, 239, 297  
Walsh J.R., Roy J., 1993, MNRAS, 262, 27  
Whelan J., Iben I.J., 1973, ApJ, 186, 1007  
Woosley S.E., & Weaver T.A., 1995, ApJS, 101, 181